Anomalous transport in correlated velocity fields

Brian Berkowitz and Harvey Scher
Department of Environmental Sciences and Energy Research, Weizmann Institute of Science, 76100 Rehovot, Israel
(Received 16 April 2009; revised manuscript received 27 October 2009; published 21 January 2010)

We examine different types of heterogeneous hydraulic conductivity fields to ascertain the basic structural features that dominate the transport behavior. We contrast two approaches to the analysis, within the framework of the continuous time random walk (CTRW), considering recent simulations of particle transport in two correlated flow fields to discern these key features. These flow fields are the steady-state solutions of Darcy flow in systems with correlated distributions, $\mathcal{P}(K(\mathbf{x}))$, of hydraulic conductivity values $K(\mathbf{x})$. One approach uses the organizational structure of the Lagrangian velocities determined from simulations to derive correlated space-time distributions for particle tracking, which are used to fit simulated breakthrough curve (BTC) data. These fits emphasize the ability to account for both early arrival times and late-time long tailing. The other approach, in this paper, treats the simulated BTCs as "measurements" and uses a truncated power-law form of $\psi(t)$, the probability density function (pdf) of local transit times, in a partial differential equation form of CTRW. Excellent fits to both data sets are obtained with a single value of β, the key parameter that characterizes the nature of the dispersive transport. The value of β is derivable from the high ξ behavior of the pdf histogram $\Phi(\xi)$ (where ξ is the inverse velocity) of the Darcy field, which determines the late-time tail within $\psi(t)$. The quality of the two fits obtained herein with a physically derived parameter set is a probe of how heterogeneous hydraulic conductivity fields with different types of correlation can affect the larger-scale transport behavior. The features that give rise to a power-law tail of local transition times and a limit of the time range for non-Fickian behavior dominate the transport. The correlation structures of the different $\mathcal{P}(K(\mathbf{x}))$ play a secondary role compared to the spectrum of less frequent events (e.g., low velocity regions) that have a large effect on the aggregate of median time transitions.

DOI: 10.1103/PhysRevE.81.011128 PACS number(s): 05.40.Fb, 05.60.−k, 02.50.−r, 05.10.Gg

I. INTRODUCTION

The characterization of highly disordered systems to enable the prediction of transport properties is an important research area in a diverse number of fields [1]. A particularly challenging type of disordered system is geological formations, which possess heterogeneity on multiple length scales. The anomalous (or non-Fickian) transport of tracers in fluid saturated geological formations indicates that effects of heterogeneities cannot be "averaged out" even on small scales. A key question in the analysis of these complex systems is what are the essential features that dominate the transport? Specifically, how is the variety of heterogeneous structures (e.g., different correlations) of these hydraulic conductivity fields linked to the degree of non-Fickian transport?

It is now well known in the literature that such a heterogeneity leads to tracer breakthrough curves (BTCs; or first passage time distributions) with power-law tailing (e.g., [2,3]). Several studies (e.g., [4–8]) have focused more specifically on the issue of discerning how specific types of heterogeneity affect the non-Fickian transport behavior, e.g., a heavy-tailed distribution of increments in log-hydraulic conductivity can yield a heavy-tailed distribution of log-velocity increments [4]. Also, it has been shown that the late-time slope of a BTC is influenced strongly by the presence of a high density of connected paths (as opposed to a random array) in the underlying hydraulic conductivity field, but is relatively insensitive to the variance of this field [8]. Recent work with particle tracking (PT) models based on the continuous time random walk (CTRW) approach has analyzed simulations based on the statistics of Lagrangian velocities of Darcy flow; the underlying flow fields were based on correlated distributions $\mathcal{P}(K(\mathbf{x}))$ of hydraulic conductivity values $K(\mathbf{x})$, where $\mathcal{P}$ denotes a (e.g., lognormal) distribution [9,10]. In this paper, we take the opportunity presented by these distinct heterogeneous $K(\mathbf{x})$ fields to reanalyze the simulations. We employ a different CTRW-based method that is based on an integro-partial differential equation (pde) to glean further insight into the structure-transport relationship.

The CTRW [11] provides a quantitative tool to incorporate distributions of local transition displacements and times into a transport framework [2,3,12,13]. The CTRW is a generalization of the familiar random walk by inserting into each step with displacement $\mathbf{s}$ a random time t drawn from a joint probability density function (pdf) $\psi(\mathbf{s},t)$. The transport process is portrayed as a sequence of these transition rates. Disordered systems characteristically have a broad distribution of rates, and statistically rare transitions of relatively long times and/or large displacements strongly affect the overall transport. The CTRW framework is effective because it incorporates the full spectrum of these rates into the transport equations.

In this framework, the challenge is to develop an accurate physical model of $\psi(\mathbf{s},t)$ for the different structures of disordered systems. Fortunately a few features of $\psi(\mathbf{s},t)$ have enabled an excellent comparison of theory to results of a wide range of laboratory experiments, field observations, and simulations (e.g., [3,14–21]). These features are the extent of a power-law region $\sim t^{-1-\beta}$, with $0<\beta<2$, the onset of the cutoff or transition region to $\beta>2$ (i.e., Fickian region), and the functional dependence of these regions on the system disorder. The incorporation of these features into a complete

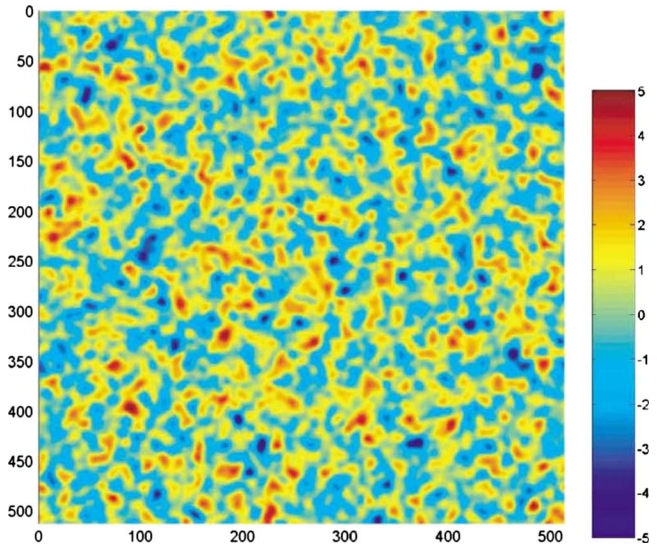

FIG. 1. (Color online) Example realization of a multilognormal hydraulic conductivity (K) field [9]. The scale to the right shows $\log_{10} K$.

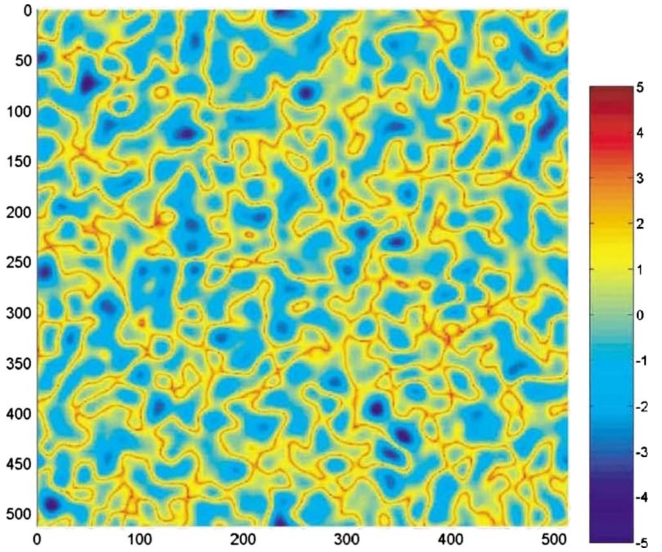

FIG. 2. (Color online) Example realization of a connected hydraulic conductivity (K) field [9]. The scale to the right shows $\log_{10} K$.

form of $\psi(\mathbf{s},t)$ (i.e., not just the limiting power-law dependence), together with other parameters in the transport equation, determines the nuances of the BTC and hence is crucial to the analysis.

II. METHODS AND RESULTS

The main method used to solve the CTRW transport equations [3] has been to transform them into pde form and use Laplace transformations $\mathcal{L}$; we discuss this below. More recently the use of PT has also proved to be powerful [9,10,22,23]. Specifically, particle transport derived from fluid flow in disordered media can be characterized statistically by (in general, coupled) distributions of transition length and particle velocities (and hence transition times). There are trade-offs between the methods. Even though very large statistical samples are needed for PT, one can work directly with the distributions and avoid $\mathcal{L}^{-1}$ of the pde approach. For the PT, the incremental steps are $\mathbf{s}^{(N+1)}=\mathbf{s}^{(N)}+\boldsymbol{\varsigma}^{(N)}$ and $t^{(N+1)}=t^{(N)}+\tau^{(N)}$, which are governed by a coupled $\psi(\mathbf{s},t)$ [14,23] and can accommodate correlations between increments [9,10]. One can also use a position-dependent $\psi(\mathbf{s},t;\mathbf{x})$ for nonstationary systems, as for the pde method [24]. All of these features are included under the basic definition of CTRW as a random walk with transition times drawn from a pdf.

In the PT approach, Le Borgne *et al.* [10] considered two types of simulated heterogeneous porous media, characterized by different correlated spatially varying hydraulic conductivity fields $\mathcal{P}(K(\mathbf{x}))$. One type is a multilognormally distributed random conductivity field with a broad range of conductivities (variance of log-conductivity =9) and a Gaussian correlation function as shown in Fig. 1. The second type of field consists of preferentially connected high conductivity zones, leading to strong localization of high velocity regions [25,26], as shown in Fig. 2. The generated fields have the same point distributions of hydraulic conductivity values and the same two-point correlation, but the connected field has more spatial organization. These two types of domains, quite different in their permeability structures, are used frequently in the hydrology literature as realistic representations of geological media [25–28]. In [10], a 512 $\times$512 grid was employed, with no-flow horizontal boundaries and flow from left to right. Incompressible fluid flow through the domains was described by the Darcy equation, while particles in each realization were subjected to motions governed by a highly idealized model. Particle trajectories were prescribed by advancing each particle according to the local advective (Darcy) flow field, together with an additional random diffusive component sampled from a Gaussian distribution. Thus, flow and transport in the domain could be treated as macroscopically one dimensional, with BTCs representing particle arrivals along a vertical control plane at a fixed distance from the inlet.

Le Borgne *et al.* [10] first solved for the velocity fields in these two types of hydraulic conductivity fields to determine the statistics of velocity correlations along a sequence of particle transitions. Particle migration was followed through the domain to generate BTCs, which can be treated as measurements, examining 100 realizations of each domain type to obtain (ensemble) averaged transport behaviors (BTCs). The velocity correlation information was then used in a CTRW-based PT algorithm. The analysis in [10] showed that the incorporation of highly detailed information on the flow field in the CTRW method, at the scale of individual particle transitions, enables fits to the "measured" BTCs that account for both early arrival times and late-time long tailing.

We shall consider these measured BTCs by employing a common pde form of the CTRW transport equations (Eqs. (24)–(26) in Ref. [3]). For our purposes we use an approximation (which will be discussed below) of a decoupled $\psi(\mathbf{s},t)=p(\mathbf{s})\psi(t)$ that yields

$$\frac{\partial c(\mathbf{s},t)}{\partial t} = -\int_0^t M(t-t')[\mathbf{v}_\psi \cdot \nabla c(\mathbf{s},t') - \mathbf{D}_\psi : \nabla\nabla c(\mathbf{s},t')]dt'. \tag{1}$$

where $c(\mathbf{s},t)$ is the normalized concentration and $M(t)$ is the memory function whose $\mathcal{L}$ is

$$\tilde{M}(u) \equiv \bar{t}u\frac{\tilde{\psi}(u)}{1-\tilde{\psi}(u)}, \tag{2}$$

with $\tilde{\psi}(u)=\mathcal{L}[\psi(t)]$ and $\bar{t}$ as a characteristic time. Here, $\mathbf{v}_\psi$ and $\mathbf{D}_\psi$ are the first and second moments of $p(\mathbf{s})$ divided by $\bar{t}$. A very useful form of $\psi(t)$, which captures simply the key features discussed above, is the truncated power law (TPL)

$$\psi(t) = N\frac{\exp(-t/t_2)}{(1+t/t_1)^{1+\beta}}, \tag{3}$$

where

$$N = [t_1\tau_2^{-\beta}\exp(\tau_2^{-1})\Gamma(-\beta,\tau_2^{-1})]^{-1}, \tag{4}$$

t_1 and t_2 are the limits of the power-law spectrum, $\tau_2 \equiv t_2/t_1$, and $\Gamma(a,x)$ is the incomplete gamma function [29]. $\mathcal{L}$ of Eq. (3) is given by

$$\tilde{\psi}(u) = (1+\tau_2 u t_1)^\beta \exp(t_1 u)\Gamma(-\beta,\tau_2^{-1}+t_1 u)/\Gamma(-\beta,\tau_2^{-1}). \tag{5}$$

The TPL form (3) of $\psi(t)$ has been used successfully to account for many laboratory-based observations [3,30–33], a field observation [17], and a behavior determined by pore-network simulation [19].

The solution of Eqs. (1)–(5) is contained in a publicly available CTRW toolbox [34]. The approximation of the decoupled form of $\psi(\mathbf{s},t)$ works well for a compact $p(\mathbf{s})$ (see discussion below) as demonstrated over a wide range of length and time scales and for diverse types of heterogeneities [3]. It also works well for the present data of a correlated permeability field, which indicates that the *time* distribution $\psi(t)$ is the essential feature. The procedure considered here uses the solution $c(\mathbf{s},t)$ to calculate the first arrival times, given by the BTC, as a function of the parameters β, t_1, and t_2 of Eq. (3)—most importantly β—and the parameters v_ψ and D_ψ in the (one-dimensional) Fokker-Planck operator in Eq. (1), which are determined by the experimental settings. To optimize the CTRW model parameters, numerical solutions were coupled to an error minimization technique that compared the solution to the simulated BTCs determined in [9,10]. More specifically, a MATLAB algorithm based on the Nelder-Mead method was used to minimize a subjective function defined as the sum of the errors between the measured and predicted values. The algorithm yielded parameters that produced good agreement between the model and data; final minor parameter value adjustments were carried out manually.

The results are shown in Figs. 3 and 4 for the two types [multilognormal and connected (Figs. 1 and 2, respectively)] of hydraulic conductivity fields. Simply stated, the essential features of the BTCs are captured by a single value of β and

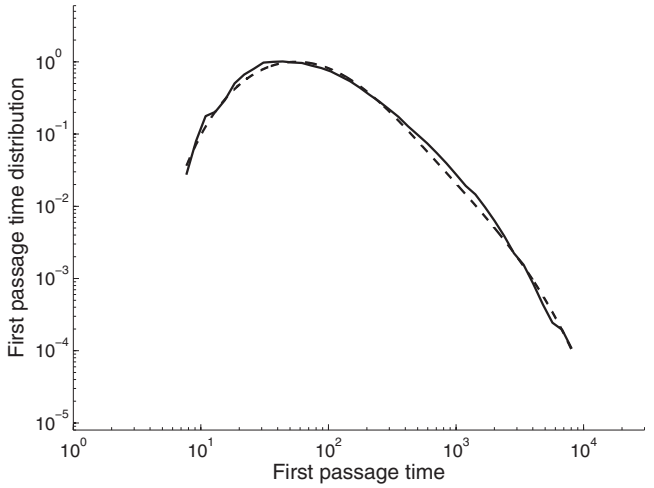

FIG. 3. First passage time distribution at a distance of 100 elements from the inlet multilognormal field, based on numerical simulations of particle tracking [10], and a fit with the CTRW using a TPL $\psi(t)$. Solid curve, numerical simulations; dashed curve, CTRW fit. The simulation curve here shows the ensemble averaged transport behavior based on 100 realizations of the underlying conductivity field. Parameters of the CTRW-TPL fit: v_ψ=2.78, D_ψ=0.49, β=1.12, $\log_{10}(t_1)$=0.15, $\log_{10}(t_2)$=3.6. Arbitrary units on v[L/T], D[L^2/T], t_1[T], and t_2[T].

by a single set of physically consistent and constrained (by the experimental parameters) values of the other parameters. The value of β is derivable from the histogram $\Phi(\xi)$ (with $\xi=1/v$) of $\mathcal{P}(K(\mathbf{x}))$ as in other studies, e.g., [17]. The estimated values of v_ψ are in accord with the average fluid velocities that can be discerned from the calculated velocity

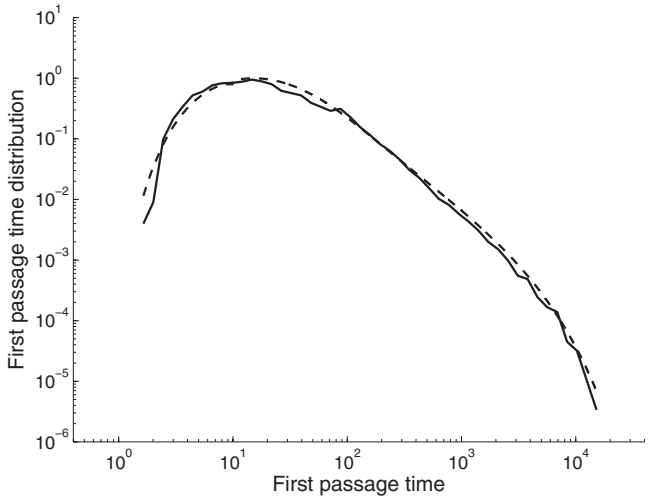

FIG. 4. First passage time distribution at a distance of 100 elements from the inlet connected field, based on numerical simulations of particle tracking [10], and a fit with the CTRW using a TPL $\psi(t)$. Solid curve, numerical simulations; dashed curve, CTRW fit. The simulation curve here shows the ensemble averaged transport behavior based on 100 realizations of the underlying conductivity field. Parameters of the CTRW-TPL fit: v_ψ=7.4, D_ψ=1.8, β=1.12, $\log_{10}(t_1)$=0.15, $\log_{10}(t_2)$=3.7. Arbitrary units on v[L/T], D[L^2/T], t_1[T], and t_2[T].

fields (Figs. 1(b) and 1(d) of [9]) in the two domains (noting also that in general the particle velocity $v_\psi \neq v$, the average fluid velocity; see [3]). Moreover, the v_ψ and D_ψ values for the multilognormal field are smaller than those for the connected field, in agreement with $\mathcal{P}(K(\mathbf{x}))$ which yields a velocity field for the multilognormal case that has a fewer connected higher velocity paths than the connected field.

The fits in Figs. 3 and 4 employ the same value of t_1, while the value of t_2 is somewhat smaller for the BTC in the multilognormal hydraulic conductivity field, indicating a transition to Fickian transport that is faster than for the connected field. The t_2 values are compatible with the value $\beta > 1$, which indicates that relative to the overall particle residence times, the domains are not highly heterogeneous [3]. The parameter t_1 simply sets the time scale and is the ratio of the characteristic displacement to the velocity, $t_1 = \bar{s}/v_\psi$. The value of $\bar{s} = c\lambda$, where $c \sim 1$ and λ is the correlation length; c is approximately 0.5 and 1.3, respectively, for the multilognormal and connected hydraulic conductivity fields [10]. In terms of robustness of the fits, changing $\log_{10} t_2$ values by, e.g., ± 0.1, yields small variations in the tail of the BTC. The other parameters (including β) display similar sensitivity to the fits, affecting early and peak arrival times in the BTCs.

III. DISCUSSION

The strength of the CTRW theory of transport in a disordered system with statistical stationarity resides in its capacity to include the most salient aspects of the interplay between different magnitudes and encounters of transitions within a broad spectrum. The basic output of most probabilistic theory is the (normalized) particle concentration $c(\mathbf{s},t)$, which is an ensemble average of all the configurations of the system. An immediate concern then arises: what is the variance of this ensemble average, i.e., what fluctuations are being neglected [3]? In the context of CTRW one can try to optimize $\psi(\mathbf{s},t)$ to include the important fluctuations. As a prime example, the typical long (power-law) tail at large times is associated with the relatively rare occurrence of low velocity regions, which tend to be uncorrelated from each other [3]. These regions provide long transition times, which can be comparable to a collection of shorter time steps produced by the higher velocities, hence, the importance of these fluctuations. From our analysis of the simulated BTCs [10] one can glean that β is a good measure of the statistics of the encounters with the long transition times present in those domains. One can see clearly the nature of the problem of transport in the Darcy flow in the $K(\mathbf{x})$ fields of Figs. 1 and 2. The point distribution of K values determines the form of $\Phi(\xi)$, which can be translated into a $\psi(t)$. The focus should thus be on the $\mathcal{P}(K(\mathbf{x}))$, $\Phi(\xi)$ relationship. The high $K(\mathbf{x})$ correlation structures in Figs. 1 and 2 are a secondary perturbation on the significant velocity spectrum. Indeed, the velocity distributions in the two domains derived from Figs. 1 and 2 were found to be very similar [9]. If $p(\mathbf{s};\mathbf{v})$ (see below) is compact, the transport is insensitive to the small ξ part of $\Phi(\xi)$.

To reiterate, it has been shown that if the pdf of displacements is compact, then the spectrum of high velocities, whether correlated or not, produces short transition times [23]. In this case the decoupled form of $\psi(\mathbf{s},t)$ is satisfactory. However, if $p(\mathbf{s})$ is Lévy-like, i.e., it has a power-law dependence on $\mathbf{s}$, then the transport is sensitive to the high velocity part of the spectrum $\Phi(\xi)$, with $\xi = 1/v$. In this case, one needs a fully coupled $\psi(\mathbf{s},t)$ because the small ξ allows a large displacement within the operational time window [23]. In a random fracture network one has a natural pdf for $\mathbf{s}$, the distribution of fracture fragments [14], via a $p(\mathbf{s};\mathbf{v})$. In a porous medium the choice for $p(\mathbf{s})$ is much more subtle. There is no obvious structural arrangement as in a random fracture network except for the pore network [19]. A natural choice for displacements relates to the dynamic aspects of the transport in a scattering medium—the velocity correlation length $\lambda(v)$. If the distribution of $\lambda(v)$ is compact then our approximation holds well. In other cases one might need a coupled $\psi(\mathbf{s},t)$.

For example, in the Lagrangian simulation approach [9] the arbitrary discretization into steps of length Δx can interfere with the extent of displacement $\lambda(v)$ at each selection of $\mathbf{v}$. The analysis in [9] in fact demonstrates that the neglect of information on the velocity correlation between the transitions of length Δx—which is linked particularly to the high velocity paths—leads to a poor fit of the early time portion of the BTC. One choice for $p(s)$ (here now used for $|\mathbf{s}|$), which is easily parametrized around the mean of the velocity correlation, is $p(s) = \mathcal{N}(\lambda(v), \Delta_\lambda)$, where $\mathcal{N}(\bar{s}, \Delta)$ is a Gaussian in the variable $\mathbf{s}$, with mean $\bar{\mathbf{s}}$ and standard deviation Δ about the mean. This pdf is part of the coupled $\psi(\mathbf{s},t) = s^{d-1} p(s) \Omega(\boldsymbol{\omega}) \frac{\Phi(t/s)}{s}$, where the angular part of $\mathbf{v}$ is contained in $\Omega(\boldsymbol{\omega})$ [23]. The choice of $\bar{s} = \lambda(v)$, which is independent of the grid size, decreases the correlation between steps, in contrast to the correlations induced by the Δx displacements. The arbitrary discretization Δx could serve as a means to determine the natural displacement $\lambda(v)$.

In general, the interpretation of simulations associated with the Lagrangian simulation approach is highly sensitive to the nature of the spatial and temporal discretizations that are employed. Moreover, such detailed and computationally intensive simulations are not readily available; it is in practice very difficult to obtain *a priori* the parameter values of $\psi(\mathbf{s},t)$, and correlations of these transitions with previous steps, in laboratory materials and/or field sites. One usually has to employ empirical best fits to the data and use independent measurements to establish consistency and/or predictions.

The pde approach applied in this paper has the merit of providing important insights into the meaning of the CTRW parameters chosen to give the best fit, in addition to not requiring detailed information on the underlying hydraulic conductivity and/or velocity fields. One such insight is derived from the fits of both BTCs in Figs. 3 and 4; these fits have the same value of β, indicating that the different high permeability pathways do not modify the statistics of the arrival times. These parameters provide agreement with additional statistical data of the simulations. Over only 2.5 decades in time, the second centered moment of the plume σ^2 "exponent" changes from 2 to 1.3 [9]. The range of the time span limits the power-law dependence. In our evaluation of σ^2 over the entire range of the BTC, the exponent changes

from 1.8 (based on the asymptotic $[\psi(t) \sim t^{-1-\beta}]$ formula $\sigma^2 \propto t^{3-\beta}$ for $1<\beta<2$) to lower values with increasing time, i.e., an approach toward 1.0 due to the effect of the transition to Fickian transport as evident in the BTC. There is a satisfactory overlap in the exponent values.

The beguilingly simple form of Eq. (3) captures some very subtle features of anomalous transport that are not readily available. The parameter t_2 determines the transition to Fickian behavior. A recent study [33] has shown how changing the time window of the experimental observation, by changing the particle velocity, shifts the time region of $\psi(t)$ that controls the nature of the transport. In some cases one can calculate t_2 [19], which was determined on the pore scale by molecular diffusion.

In general, in the absence of detailed information of $K(\mathbf{x})$, as is the case in many of the studies in the literature using CTRW, one can have confidence that the parameters used in the fit are a meaningful expression of the important fluctuations of transport in the Darcy velocity field generated by $K(\mathbf{x})$. In the present case, one can use the result of the fits in Figs. 3 and 4 that specify Eq. (3) and make predictions, e.g., to examine the consequence of reducing the mean flow (cf. [33]).

IV. CONCLUSION

The results presented here—an excellent fit of the simulation data with a single value of β and other physically consistent and constrained values—imply that the distribution of local transition *times*, derived from a statistically sufficient disorder of the medium—promoting a broad range of different velocity locales—is the dominant factor controlling the transport. This spectrum of times as the mechanism for transport in disordered systems occurs in many different contexts, e.g., [35]. The statistical similarity of the two $\mathcal{P}(K(\mathbf{x}))$ is generated by the same point distributions of hydraulic conductivity values and the same two-point correlation. The extent of the disorder determines both β and t_2, the latter of which in this case influences the BTC tail in Figs. 3 and 4. Significantly, these results cast doubt on the ability to discern how heterogeneous hydraulic conductivity fields with different types of correlation can affect the larger-scale transport behavior. These results also exemplify the difficulty in attempting to identify different heterogeneous structures of hydraulic conductivity fields solely on the basis of BTC analysis. We find that a compact $p(\mathbf{s})$ is adequate, which implies that the spectrum of high velocities—whether correlated or not—plays a secondary role. It is to be emphasized that the hydraulic conductivity fields studied herein are generated by two probability distributions $\mathcal{P}(K(\mathbf{x}))$ that promote a high degree of statistical stationarity (assuming modest correlation lengths). In natural geological formations the heterogeneity can be considerably more complicated (e.g., with long-range correlations) and features dominating the transport could involve the use of more extended theoretical aspects such as a position-dependent $\psi(\mathbf{s},t;\mathbf{x})$ [24].

ACKNOWLEDGMENTS

The authors thank Tanguy Le Borgne for supplying the data files from the numerical simulations. The financial support of the European Commission (Contract No. PITN-GA-2008-212298) is gratefully acknowledged.

[1] D. ben Avraham and S. Havlin, *Diffusion and Reactions in Fractals and Disordered Systems* (Cambridge University Press, Cambridge, England, 2000).
[2] R. Metzler and J. Klafter, Phys. Rep. **339**, 1 (2000).
[3] B. Berkowitz, A. Cortis, M. Dentz, and H. Scher, Rev. Geophys. **44**, RG2003 (2006).
[4] M. V. Kohlbecker, S. W. Wheatcraft, and M. M. Meerschaert, Water Resour. Res. **42**, W04411 (2006).
[5] A. Fiori, I. Janković, G. Dagan, and V. Cvetković, Water Resour. Res. **43**, W07445 (2007).
[6] D. Fernàndez-Garcia and J. J. Gómez-Hernández, Water Resour. Res. **43**, W02423 (2007).
[7] M. Rhodes, B. Bijeljic, and M. J. Blunt, Adv. Water Resour. **31**, 1527 (2008).
[8] M. Willmann, J. Carrera, and X. Sanchez-Vila, Water Resour. Res. **32**, W12437 (2009).
[9] T. Le Borgne, M. Dentz, and J. Carrera, Phys. Rev. E **78**, 026308 (2008).
[10] T. Le Borgne, M. Dentz, and J. Carrera, Phys. Rev. Lett. **101**, 090601 (2008).
[11] E. W. Montroll and G. H. Weiss, J. Math. Phys. **6**, 167 (1965).
[12] H. Scher and M. Lax, Phys. Rev. B **7**, 4491 (1973).
[13] H. Scher and E. W. Montroll, Phys. Rev. B **12**, 2455 (1975).
[14] B. Berkowitz and H. Scher, Phys. Rev. E **57**, 5858 (1998).
[15] Y. Hatano and N. Hatano, Water Resour. Res. **34**, 1027 (1998).
[16] G. Drazer, M. Rosen, and D. H. Zanette, Physica A **283**, 181 (2000).
[17] G. Di Donato, E.-O. Obi, and M. J. Blunt, Geophys. Res. Lett. **30**, 1608 (2003).
[18] A. Cortis, Y. Chen, H. Scher, and B. Berkowitz, Phys. Rev. E **70**, 041108 (2004).
[19] B. Bijeljic and M. J. Blunt, Water Resour. Res. **42**, W01202 (2006).
[20] X. X. Zhang and M. C. Lv, Water Resour. Res. **43**, W07437 (2007).
[21] A. Zoia, Phys. Rev. E **77**, 041115 (2008).
[22] M. Dentz, A. Cortis, H. Scher, and B. Berkowitz, Adv. Water Resour. **27**, 155 (2004).
[23] M. Dentz, H. Scher, D. Holder, and B. Berkowitz, Phys. Rev. E **78**, 041110 (2008).
[24] A. Cortis, C. Gallo, H. Scher, and B. Berkowitz, Water Resour. Res. **40**, W04209 (2004).
[25] B. Zinn and C. F. Harvey, Water Resour. Res. **39**, 1051 (2003).
[26] C. Knudby and J. Carrera, J. Hydrol. **329**, 377 (2006).
[27] P. Salandin and V. Fiorotto, Water Resour. Res. **34**, 949 (1998).
[28] T. Ouellon, R. Lefebvre, D. Marcotte, A. Boutin, V. Blais, and M. Parent, J. Hydrol. **351**, 71 (2008).

[29] M. Abramowitz and I. Stegun, *Handbook of Mathematical Functions* (Dover, New York, 1970).
[30] B. Berkowitz, H. Scher, and S. E. Silliman, Water Resour. Res. **36**, 149 (2000).
[31] Y. W. Xiong, G. H. Huang, and Q. Z. Huang, J. Contam. Hydrol. **86**, 163 (2006).
[32] J. C. Deng, X. Jiang, X. X. Zhang, W. Hu, and J. W. Crawford, Chemosphere **71**, 2150 (2008).
[33] B. Berkowitz and H. Scher, Adv. Water Resour. **32**, 750 (2009).
[34] B. Berkowitz and Group, CTRW MATLAB TOOLBOX, ESER, 2008.
[35] I. Golding and E. C. Cox, Phys. Rev. Lett. **96**, 098102 (2006).